JOURNAL OF AGRICULTURAL AND FOOD CHEMISTRY

J. Agric. Food Chem. **2008,** *56,* 59–62 **59**

On the Diffusion Constant of Water in Wheat

MARCO L. H. GRUWEL,*,†,‡ PRABAL K. GHOSH,§ PETER LATTA,†,|| AND DIGVIR S. JAYAS§

NRC Institute for Biodiagnostics, 435 Ellice Avenue, Winnipeg, Manitoba R3B 1Y6, Canada, Department of Chemistry, University of Manitoba, Winnipeg, Manitoba R3T 2N2, Canada, Department of Biosystems Engineering, University of Manitoba, Winnipeg, Manitoba R3T 5V6, Canada, and Institute for Measurement Science, Slovak Academy of Sciences, Dúbravská cesta 9, SK-84219 Bratislava, Slovakia

Diffusion-weighted magnetic resonance imaging (MRI) was used to obtain diffusion constants for water in the embryo and endosperm of wheat. Our experiments showed a significant difference between the diffusion constant for the two components. It was also shown that water diffusion in both the endosperm and embryo deviates from the typically observed Gaussian behavior in bulk fluids, showing a time-dependent diffusion constant. Diffusion constants for the embryo and endosperm were shown to differ by an order of magnitude. Using a model for restricted diffusion, information on the endosperm pore size and the embryo cell dimensions could be obtained.

KEYWORDS: Moisture; MRI; diffusion; spin–echo; pulsed gradients; restricted mobility

1. INTRODUCTION

Usually grains are harvested at a moisture content that is too high for safe long-term storage, for example, to prevent shattering loss. To prepare for storage, grains must thus be subjected to a drying process using heated or ambient forced air. Details of the drying process depend upon the initial moisture content and the projected storage time (*1, 2*).

Drying can be described as a combination of internal mass and heat transfer caused by a concentration gradient resulting from a liquid to vapor transformation, typically at the grain surface. Different mathematical models have been presented for the study of drying grains (*3–6*), and a summary of these models has been given by Miketinac et al. (*7*). The method of choice to solve the sets of coupled differential equations in these models is the finite element analysis (*8*). These models assume that moisture transfer to the kernel surface is facilitated by diffusion of water, in the form of liquid or vapor, and were derived using a number of assumptions to simplify these models for computation. All models assumed the initial moisture distribution within the grain kernel to be uniform. During drying, no compartmentation within the kernels was considered.

However, it is known from recent magnetic resonance imaging (MRI) studies that the water distribution in seeds is nonuniform, prior to and during drying (*9–11*). These experiments showed that during drying moisture loss from the kernel can be described as a nonuniform process. Individual components of the kernels played an important role in the drying process as was shown in experiments with mechanically scarified kernels and kernels without embryo (*10*). Calculations modeling the drying process of grains are thus hampered by an oversimplification of the input parameters. Using MRI, the inhomogeneous water distribution in grain kernels can be followed over time. The resulting data can be used as input for model calculations. Unfortunately, accurate diffusion data of the different grain components are not available, resulting in simplifications that do not represent reality, reducing the accuracy of the model predictions.

The aim of this work is to obtain water diffusion constants for the different grain components using pulsed field gradient (PFG) MRI (*12*). Although an extremely useful tool in material science, PFG MRI has only sporadically been used to obtain water diffusion constants from the major seed components at different moisture contents (*13–15*).

2. MATERIALS AND METHODS

2.1. Instrumentation. All MRI experiments were performed on a 11.7 T (500 MHz) Magnex (Magnex Scientific Ltd., Yarnton, U.K.) vertical bore magnet equipped with a Magnex SGRAD 123/72/S 72 mm self-shielded, water-cooled gradient set, producing a maximum gradient strength of 600 mT m^{-1}. A Bruker (Milton, Ontario, Canada) Avance DRX console with a ParaVision 3.0.2 operating system was interfaced to the magnet. The probe and coil (Helmholtz configuration; 7 mm i.d.) were home-built. All experiments were performed at room temperature (20.5 ± 0.5 °C).

2.2. Sample Handling. Prior to imaging, two separate batches of A.C. Barrie (*Triticum aestivum* L.) wheat kernels were preconditioned to a selected moisture content by imbibition for 14–16 h in distilled water. The final moisture content of the batches was 39.3 ± 0.9% wb. This value was selected to allow for MRI experiments with a relatively

* To whom correspondence should be addressed. E-mail: marco.gruwel@nrc-cnrc.gc.ca.
† NRC Institute for Biodiagnostics.
‡ Department of Chemistry, University of Manitoba.
§ Department of Biosystems Engineering, University of Manitoba.
|| Slovak Academy of Sciences.

10.1021/jf0720537 CCC: $40.75
Published on Web 12/11/2007

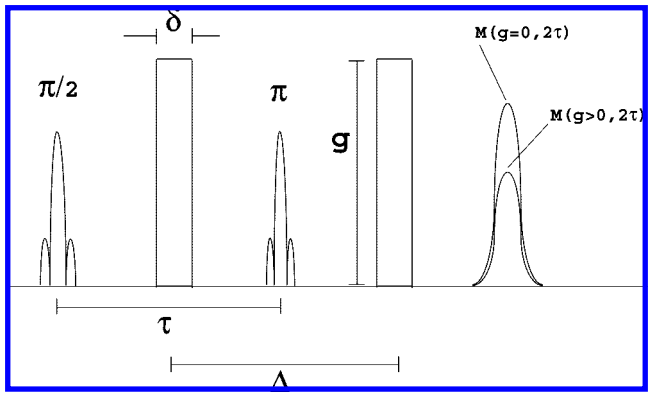

Figure 1. PFG spin–echo experiment. Only the pulsed gradients and the radio frequency (RF) are shown. Δ corresponds to the time between the gradient pulses; δ corresponds to the duration of the gradient pulses; and g corresponds to the amplitude of the gradients. The echo is created at 2τ using slice-selective Hermite RF pulses.

high signal-to-noise ratio. Of each batch, 4 kernels ($n = 4$) were selected for MRI. For microimaging, the imbibed seeds were carefully surface-dried using a paper towel. After drying, the seed was glued onto the inner surface of a small glass cylinder (7 mm o.d.), which could be inserted into the probe. Both ends of the glass cylinder were sealed with Parafilm (American Can Comp., Greenwich, CT) to avoid possible drying during the MRI experiment. Immediately after insertion into the probe, the seed was imaged. For both batches average seed moisture levels were determined with the standard ASAE procedure for unground grain and seeds [American Society of Agricultural Engineers (ASAE) S352.2] (*16*).

2.3. Microimaging. Images were obtained using a conventional 2D spin–echo sequence with PFGs symmetrically positioned around the refocusing pulse and applied in the read-out direction (see **Figure 1**). The excitation and refocusing pulse both had a Hermite shape and durations of 1000 and 633 μs, respectively. Time of echo (TE) was kept at a minimum and varied from 10.8 to 20.8 ms, depending upon the separation between the two gradient pulses (Δ), and time of repetition (TR) was 500 ms. The duration (δ) of the pulsed gradients was kept small and fixed at 2 ms. The PFGs were oriented along the frequency-encode direction. Images were acquired as a 128 × 128 data matrix with a field of view (FOV) of 1.28 × 1.28 cm^2 for a 2.4 mm thick slice. Each experiment was composed of two averages for each value of the pulsed gradients. In total, seven different gradient strengths were used, varying from 5 to a maximum value of 600 mT m^{-1}. Typically, these experiments took 17 min each to acquire. The temperature in the probe was 20.5 ± 0.5 °C.

2.4. Statistics. Data in this study are represented as means ± standard deviation. The number data averaged is indicated by n.

2.5. Theory. In diffusion PFG MRI experiments, the diffusion constant of the spin carrier is defined as the mean-square displacement in the direction of the pulsed gradients per unit time

$$\frac{\langle[\vec{r}'(t) - \vec{r}(0)]^2\rangle}{t} = 2dD(t) \tag{1}$$

where d represents the dimensionality of the system (d = 1–3) and $D(t)$ represents the time-dependent diffusion constant. The PFG MRI experiment provides information on diffusion over a wide time scale (*12*). The modulation of the echo amplitude in the presence of a time-dependent gradient $g(t)$ is given by

$$M(g,2\tau) = M(0,2\tau)\exp\left(-\gamma^2 D(t)\left[\int_0^{2\tau}\left(\int_0^{t'} g(t'')\mathrm{d}t''\right)^2\mathrm{d}t'\right]\right) \tag{2}$$

Application of two gradient pulses of duration δ, amplitude g, and separation Δ, symmetrically positioned around the refocusing pulse, provides an attenuation of the spin–echo amplitude at a time 2τ (see **Figure 1**). Here, we assume that the effect of background gradients is negligible compared to the effects of the much stronger pulsed gradients. For bulk fluids, it can be shown that this modulation of the spin–echo amplitude ($M(g, 2\tau)$) is simply given by

$$M(g,2\tau) = M(0,2\tau)\exp\left(-\gamma^2\delta^2 D_0 g^2\left(\Delta - \frac{\delta}{3}\right)\right)$$
$$M(g,2\tau) = M(g,\Delta) \tag{3}$$

The echo attenuation can thus be used to obtain the bulk diffusion constant (time-independent) $D(t) = D_0$. As soon as the propagation of water molecules cannot be described by a Gaussian distribution, which describes the motion of water in bulk fluids, eq 3 no longer holds. This situation arises when studying the diffusion of water in small cavities, such as porous rocks (*17*), when the diffusion of spins is restricted before significant dephasing has occurred, i.e., in the presence of weak gradients and a physical confinement to a small volume.

Mitra et al. (*18, 19*) have shown that for short times ($\sqrt{D_0 t} \ll l_p$, with l_p being a typical pore size) using the appropriate propagator for diffusion in a restricted system, the diffusion constant is time-dependent ($D(t)$) and is related to the bulk value D_0 by

$$D(t) = D_0\left(1 - \frac{4}{9\sqrt{\pi}}\frac{S}{V}\sqrt{D_0 t}\right) + O(D_0 t) \tag{4}$$

where S and V represent surface and volume, respectively, of the cavity. In a PFG experiment, t will be replaced by Δ for the diffusion weighting of the MRI signal and $D(t) = \Delta$ is the time-dependent diffusion coefficient fitted to eq 3. In general, eq 4 shows that for short times the diffusion constant is independent of the exact details of the restricting geometry and only depends upon the surface/volume ratio (S/V) of the occupied space. Biological systems often show no or a very small time dependence of the diffusion constant because of the rather large value of S/V. The diffusion constant quickly decays to an effective value, which becomes independent of S/V. In this case, the long-time limit has been reached (*17*). In this limit, the diffusion coefficient is given by

$$D(t) = D_0\left(\frac{1}{\alpha} + \frac{\beta}{D_0 t}\right) + O\left((D_0 t)^{-\frac{3}{2}}\right) \tag{5}$$

where $1/\alpha$ represents tortuosity and β represents a parameter describing the microscopic character of the sample. At present, no theory exists for the diffusion constant in the intermediate time regime. However, eqs 4 and 5 are series expansions of the diffusion constant in a series of $\sqrt{t}$. When the two limits are known, a Padé approximation can be used to interpolate for intermediate times between the extremes (*17, 20*)

$$D(t) = D_0\left(1 - \left(1 - \frac{1}{\alpha}\right)\left[\frac{c\sqrt{t} + \left(1 - \frac{1}{\alpha}\right)\frac{t}{\theta}}{\left(1 - \frac{1}{\alpha}\right) + c\sqrt{t} + \left(1 - \frac{1}{\alpha}\right)\frac{t}{\theta}}\right]\right) \tag{6}$$

where $c = (4/9\sqrt{\pi})(S/V)\sqrt{D_0}$ and θ has the dimension of time.

Using Mitra's theory, we will obtain the diffusion of water in wheat for the two time limits, using eq 6 to fit our data. Using this approach, effective diffusion constants and values for S/V, the surface/volume ratio of the pore, can be obtained.

3. RESULTS AND DISCUSSION

Figure 2 shows the diffusion constant as a function of the diffusion time, Δ, for wheat with a moisture content of 39.3% wb. For D_0, the diffusion constant of bulk water at 20.5 ± 0.5 °C, we used a value of 220 × 10^{-5} mm^2 s^{-1}. Using Origin7.0 (OriginLab Corporation, Northampton, MA), the diffusion time dependence of the diffusion constant $D(t)$ was fit to eq 6 to obtain α, c, and θ for both the embryo and endosperm. Data fitting was performed using the Marquardt–Levenberg algorithm to minimize X^2, and the results are listed in **Table 1**.

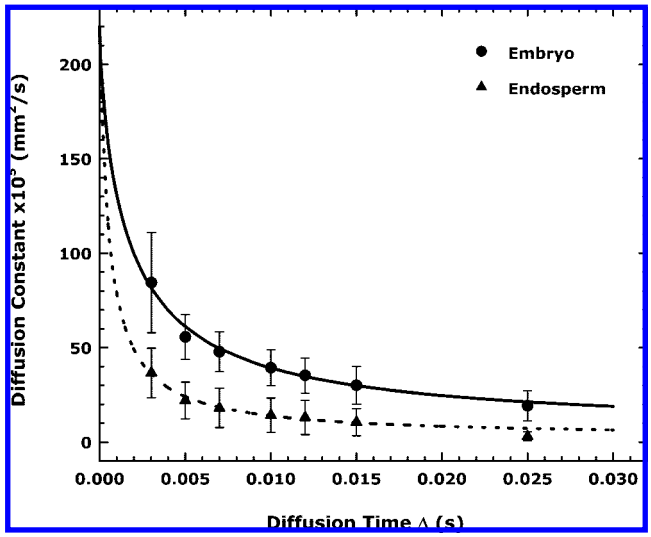

Figure 2. Plot of the apparent water diffusion coefficient as a function of the diffusion time (Δ) at 20.5 ± 0.5 °C for wheat kernels with an average moisture level of 39.3% wb ($n = 8$). The solid and dotted lines represent a fit of the data to eq 6 for the embryo and endosperm, respectively. The values obtained from the fit are listed in **Table 1**.

Table 1. Parameters Obtained from Fitting eq 6 to the Data of the 39.3% wb Moisture Level Seeds ($n = 8$) (**Figure 2**)

39.3% wb A.C. Barrie wheat			
embryo		endosperm	
α	38.33 ± 0.96	α	86.2 ± 4.7
c	7.82 ± 0.11 ($s^{-1/2}$)	c	2.26 ± 0.83 ($s^{-1/2}$)
θ	2.180 ± 0.008 × 10^{-3} (s)	θ	0.560 ± 0.004 × 10^{-3} (s)

The diffusion constant of water in wheat is time- and component-dependent, as shown in **Figure 2**. The difference between the diffusion constants for the embryo and endosperm is largest for small values of the diffusion time, Δ. Values of the diffusion constant needed for processes on macroscopic time scales, such as the drying process, can be calculated as

$$\lim_{t\to\infty} D(t) = D_{\text{app}} = \frac{D_0}{\alpha} \tag{7}$$

For the diffusion constant of water in the wheat embryo, we obtained $D^{\text{app}} = (5.7 \pm 0.2) \times 10^{-5}$ mm^2 s^{-1} for the 39.3% wb moisture level. Water diffusion in wheat endosperm was observed to be slower compared to water in the embryo, $D^{\text{app}} = (2.6 \pm 0.2) \times 10^{-5}$ mm^2 s^{-1}.

Previous MRI reports on water diffusion in wheat (*13, 14*) report water diffusion coefficients approximately an order of magnitude higher than the values reported here. For endosperm, Eccles et al. report a diffusion constant of (50–70) × 10^{-5} mm^2 s^{-1} (*14*). This value is likely high because the Δ dependence of the echo attenuation of the MRI experiment was not considered. From **Figure 2**, it is clear that such high values for the water diffusion constant in the endosperm can be observed for short values for Δ. Kang et al. report diffusion constants for water in the endosperm for different wheat varieties that are much closer [(0.4–2.9) × 10^{-5} mm^2 s^{-1}] to the values calculated by us in this work (*21, 22*). The diffusion constant was obtained fitting analytical solutions to the diffusion equation to the water uptake data acquired using the air-oven method. Literature on the diffusion constant of water in the wheat embryo is scarce. Measurement of the water diffusion constant for cell-associated water in the embryo of ripening barley seeds at 25 °C has been reported (*15*). The MRI experiments also showed the Δ dependence of the diffusion constant as observed by us; however, no interpretation of this observation was provided. The values reported ranged from approximately 200 to 20 × 10^{-5} mm^2 s^{-1}. The higher end of this range approaches the diffusion constant of bulk water at 25 °C.

The short-time transient behavior of the diffusion constant, according to eq 6, allows one to extract valuable information on the geometry of the component in which the water molecules diffuse. This would provide valuable information on the porosity of the endosperm, which mainly consists of starch. **Table 1** lists the values for the parameter c in the Padé approximant given in eq 6. Using this parameter, the surface/volume ratio for the pore or component can be estimated. For the endosperm, we obtained $S/V = 192 \pm 70$ mm^{-1} for the 39.3% wb moisture samples. The surface/volume ratio for the compartments in the embryo was calculated to be 665 ± 9 mm^{-1}. Assuming that the pores have an approximate spherical shape, the radius, R, of the pores can be calculated from

$$\frac{S}{V} = \frac{3}{R} \tag{8}$$

For the endosperm, we obtained a pore space radius of $R = 15.6 \pm 5.7$ μm, and for the embryo, we obtained a pore space radius of $R = 4.51 \pm 0.06$ μm, for the 39.3% wb moisture samples.

A recent study on starch pore sizes reported an average pore diameter of approximately 57 μm for wheat starch (*23*). It should be noticed that this value represents an average of a broad distribution, depending upon the source and plant genotype. A study including multiple varieties grown at various locations and under different cultivation intensities shows that the largest volume fraction of starch granules contains particles in the size range (diameter) of 10–50 μm (*24*). Knowing that the granule size approximately corresponds to the pore size, our result of an approximately 30 μm pore diameter thus appears to be a reasonable one for our sample of A.C. Barrie wheat.

The wheat embryo mainly consists of cells. During exposure to water (humidity), these cells rehydrate. Water diffusion measurements of the embryo thus relate to water movement within these cells. For simplicity assuming spherical cells, the diffusion measurements indicate the presence of cells with an average length of approximately 9 μm. Optical microscopy of wheat embryos showed cells with dimensions smaller than 10 μm (*25*). The value reported in this work is in line with the optical microscopy data on isolated embryos.

In conclusion, we have shown that diffusion-weighted MRI can be used to obtain diffusion constants of water inside seeds. These measurements provide valuable information on the geometry (S/V) of the water reservoirs in the seeds.

ABBREVIATIONS USED

FOV, field of view; MRI, magnetic resonance imaging; RF, radio frequency; TE, time of echo; TR, time of repetition; PFG, pulsed field gradient.

LITERATURE CITED

(1) Brooker, D. B.; Bakker-Arkema, F. W.; Hall, C. W. *Drying and Storage of Grains and Oilseeds*; Van Nostrand Reinhold: New York, 1992.

(2) Pabis, S.; Jayas, D. S.; Cenkowski, S. *Grain Drying: Theory and Practice*; John Wiley and Sons, Inc.: New York, 1998.

(3) Jia, C. C.; Sun, D. A.; Cao, C. W. Mathematical simulation of temperature and moisture fields within a grain kernel during

drying. *Drying Technol.* **2000**, *18* (6), 1305–1325.
(4) Neményi, M.; Czaba, I.; Kovacs, A.; Jani., T. Investigation of simultaneous heat and mass transfer within the maize kernels during drying. *Comp. Elect. Agric.* **2000**, *26* (2), 123–135.
(5) Sokhansanj, S.; Gustafson, R. J. Prediction of heat and mass transfer within a grain kernel a finite element application. In *Drying 80*; Majumdar, A. S., Ed.; McGraw-Hill International Book Company: New York, 1980; Vol. 2, pp 229–232.
(6) Yang, W.; Jia, C. C.; Siebenmorgen, T. J.; Howell, T. A.; Cnossen, A. G. Intra-kernel moisture responses of rice to drying and tempering treatments by finite element simulation. *Trans. ASAE* **2002**, *45* (4), 1037–1044.
(7) Miketinac, M. J.; Sokhansanj, S.; Tutek, Z. Determination of heat and mass transfer coefficients in thin layer drying of grain. *Trans. ASAE* **1992**, *35* (6), 1853–1858.
(8) Segerlind, L. J. *Applied Finite Element Analysis*, 2nd ed.; John Wiley and Sons, Inc.: New York, 1984.
(9) Song, H. P.; Litchfield, J. B.; Morris, H. D. Three dimensional microscopic MRI of maize kernels during drying. *J. Agric. Eng. Res.* **1992**, *53* (1), 51–69.
(10) Ghosh, P. K.; Jayas, D. S.; Gruwel, M. L. H.; White, N. D. G. Magnetic resonance image analysis to explain moisture movement during wheat drying. *Trans. ASABE* **2006**, *49* (4), 1181–1191.
(11) Kovács, A. J.; Neményi, M. Moisture gradient vector calculation as a new method for evaluating NMR images of corn (*Zea mays* L.) kernels during drying. *Magn. Reson. Imaging* **1999**, *17* (7), 1077–1082.
(12) Stejskal, E. O.; Tanner, J. E. Spin diffusion measurements: Spin echoes in the presence of a time-dependent field gradient. *J. Chem. Phys.* **1965**, *42*, 288–292.
(13) Callaghan, P. T.; Jolley, K. W.; Lelievre, J. Diffusion of water in the endosperm tissue of wheat grains as studied by pulsed field gradient nuclear magnetic resonance. *Biophys. J.* **1979**, *28* (1), 133–142.
(14) Eccles, C. D.; Callaghan, P. T.; Jenner, C. F. Measurement of the self-diffusion coefficient of water as a function of position in wheat grain using nuclear magnetic resonance imaging. *Biophys. J.* **1988**, *53* (1), 77–81.
(15) Ishida, N.; Ogawa, H.; Kano, H. Diffusion of cell-associated water in ripening barley seeds. *Magn. Reson. Imaging* **1995**, *13* (5), 745–751.
(16) ASAE moisture measurement—Unground grain and seeds. In *Standards 1996*; American Society of Agricultural Engineers (ASAE): St. Joseph, MI, 1996; p 387.
(17) Sen, P. N. Time-dependent diffusion coefficient as a probe of geometry. *Concepts Magn. Reson.* **2004**, *23* (1), 1–22.
(18) Mitra, P. P.; Sen, P. N.; Schwartz, L. M.; Le Doussal, P. Diffusion propagator as a probe of the structure of porous materials. *Phys. Rev. Lett.* **1992**, *68* (24), 3555–3558.
(19) Latour, L. L.; Svoboda, K.; Mitra, P. P.; Sotak, C. H. Time-dependent diffusion of water in a biological model system. *Proc. Natl. Acad. Sci. U.S.A.* **1994**, *91*, 1229–1233.
(20) Latour, L. L.; Mitra, P. P.; Kleinberg, R. L.; Sotak, C. H. Time-dependent diffusion coefficient of fluids in porous media as a probe of surface-to-volume ratio. *J. Magn. Reson.* **1993**, *101*, 342–346.
(21) Kang, S.; Delwiche, S. R. Moisture diffusion modelling of wheat kernels during soaking. *Trans. ASABE* **1999**, *42* (5), 1359–1365.
(22) Kang, S.; Delwiche, S. R. Moisture diffusion coefficients of single wheat kernels with assumed simplified geometries: Analytical approach. *Trans. ASABE* **2000**, *43* (6), 1653–1659.
(23) Fortuna, T.; Januszewska, R.; Juszczak, L.; Kielski, A.; Pałasinski, M. The influence of starch pore characteristics on pasting behaviour. *Int. J. Food Sci. Technol.* **2000**, *35*, 285–291.
(24) Capouchová, I.; Petr, J.; Marešová, D. Evaluation of size distribution of starch granules in selected wheat varieties by the low-angle laser light scattering method. *Plant Soil Environ.* **2003**, *49* (1), 12–17.
(25) Zhang, D. M.; Lin, Y. B.; Cui, F. Z.; Tian, M. B. Morphological evolution of embryonic cells of wheat seeds upon low-energy ions. *Mater. Sci. Eng., C* **2000**, *11*, 75–79.

Received for review July 9, 2007. Revised manuscript received October 15, 2007. Accepted October 19, 2007. We thank the Canada Research Chairs program for funding this study.

JF0720537